

## Video Article

# RiboTag Immunoprecipitation in the Germ Cells of the Male Mouse

Lauren G. Chukrallah<sup>1</sup>, Kelly Seltzer<sup>1</sup>, Elizabeth M. Snyder<sup>1</sup><sup>1</sup>Department of Animal Science, Rutgers UniversityCorrespondence to: Elizabeth M. Snyder at [elizabeth.snyder@rutgers.edu](mailto:elizabeth.snyder@rutgers.edu)URL: <https://www.jove.com/video/60927>DOI: [doi:10.3791/60927](https://doi.org/10.3791/60927)

Keywords: Developmental Biology, Issue 157, cell-specific, male germ cell, RNA, RiboTag, Ribosome, translation, spermatogenesis

Date Published: 3/4/2020

Citation: Chukrallah, L.G., Seltzer, K., Snyder, E.M. RiboTag Immunoprecipitation in the Germ Cells of the Male Mouse. *J. Vis. Exp.* (157), e60927, doi:10.3791/60927 (2020).

## Abstract

Quantifying differences in mRNA abundance is a classic approach to understand the impact of a given gene mutation on cell physiology. However, characterizing differences in the translome (the whole of translated mRNAs) provides an additional layer of information particularly useful when trying to understand the function of RNA regulating or binding proteins. A number of methods for accomplishing this have been developed, including ribosome profiling and polysome analysis. However, both methods carry significant technical challenges and cannot be applied to specific cell populations within a tissue unless combined with additional sorting methods. In contrast, the RiboTag method is a genetic-based, efficient, and technically straightforward alternative that allows the identification of ribosome associated RNAs from specific cell populations without added sorting steps, provided an applicable cell-specific *Cre* driver is available. This method consists of breeding to generate the genetic models, sample collection, immunoprecipitation, and downstream RNA analyses. Here, we outline this process in adult male mouse germ cells mutant for an RNA binding protein required for male fertility. Special attention is paid to considerations for breeding with a focus on efficient colony management and the generation of correct genetic backgrounds and immunoprecipitation in order to reduce background and optimize output. Discussion of troubleshooting options, additional confirmatory experiments, and potential downstream applications is also included. The presented genetic tools and molecular protocols represent a powerful way to describe the ribosome-associated RNAs of specific cell populations in complex tissues or in systems with aberrant mRNA storage and translation with the goal of informing on the molecular drivers of mutant phenotypes.

## Video Link

The video component of this article can be found at <https://www.jove.com/video/60927/>

## Introduction

Analysis of a cell or tissue's RNA abundance, as examined by microarray or RNA-sequencing, has proven a powerful tool to understand the molecular drivers of mutant phenotypes. However, these relatively incomplete analysis tools may not inform on the physiology or proteome of the cell, especially in systems where many mRNAs are stored prior to translation such as neural and germ cells. In these systems, defining the population of mRNAs being actively translated into protein, or the cell's translome, may be a better indicator of the cell's actual physiological state<sup>1,2</sup>. For example, germ cells at various stages of development transcribe RNAs that are stored for later translation, driven either by developmental<sup>3</sup> or signaling cues<sup>4</sup>. This process is exemplified by the mRNAs encoding protamines, wherein the mRNA transcript is detectable days before the protein is made<sup>1,2,5,6</sup>. Likewise, neural cells transcribe RNA in the nucleus and transport it down the axon, as is the case with  $\beta$ -actin<sup>7</sup>. In addition to these specialized cell systems, steady-state transcriptomes are unlikely to be informative in models where RNA storage, ribosome biogenesis, or mRNA translation are impacted. Multiple other factors may also impact a cell's steady-state RNA pool include mRNA decay and the activity of RNA binding proteins. In these cases, robust tools to analyze ribosome-associated RNAs or mRNAs under active translation are more likely to yield biologically relevant results.

To that end, several methods have been developed for identifying ribosome-associated or actively translated messages. Polysome profiling, which provides a snapshot of ribosome associated transcripts, has been used for many decades to isolate intact RNAs associated with either ribosomal subunits or mono-, di-, and poly-ribosome complexes<sup>3</sup>. Briefly, collected cell lysates are applied to a linear sucrose gradient and centrifuged as high speed, resulting in separation of the ribosome subunits, intact ribosomes, and polysomes by size. Traditionally, this technique has been applied to study one or a few mRNAs, but recently this method has been combined with RNA-seq studies to elucidate the function of potential translational regulators<sup>8,9</sup>. While a powerful way to differentiate between actively translating and non-translating mRNAs<sup>10</sup>, polysome profiling does require time-consuming methods (gradient fractionation and ultracentrifuge) and can require a good deal of sample making the analysis of rare cell populations challenging.

An alternative approach to examining the translome is ribosome profiling, which identifies the portions of transcripts directly associated with the ribosome. In brief, ribosome associated RNA fragments are generated via RNase protection assay, individual ribosome complexes separated via sucrose gradient, and associated RNA fragments isolated and converted to RNA-seq tags amenable to deep sequencing<sup>11</sup>. One of the key benefits to ribosome profiling is the ability to determine the specific locations of the ribosomes at the time of isolation which allows identification of translation start sites, calculation of ribosomal occupancy and distribution, and identification of ribosome stalls<sup>12</sup>. However, this method has several inherent drawbacks, including equipment needs (gradient fractionator and ultracentrifuge), a relatively complex protocol that require

extensive troubleshooting, and computational issues not easily handled by the inexperienced user<sup>11</sup>. Importantly, ribosome profiling is primarily applied to isolated cells in culture and requires substantial material, making its application to mixed cell-type tissues or sorted cells from in vivo limited.

The mammalian RiboTag method, developed by Sanz et al. in 2009<sup>13</sup>, eliminates a number of issues inherent to both polysome and ribosome profiling. In this method, ribosome-associated RNAs can be isolated from specific cell types allowing for investigation of cell-type specific translomes in complex tissues without additional isolation techniques and specialized equipment, as is necessary in other methods<sup>13,14</sup>. The basis of the RiboTag method is a transgenic mouse model (RiboTag) carrying a modified locus for the 60S ribosomal subunit protein gene *Rpl22*. This locus (*Rpl22-HA*) includes a floxed terminal exon followed by an additional copy of the terminal exon amended to include a C-terminal hemagglutinin (HA) tag within the coding region. When crossed to a mouse expressing a cell-specific *Cre* Recombinase, the floxed exon is removed allowing the expression of HA-tagged RPL22 in a cell-specific manner (Figure 1). The HA tag can then be used to immunoprecipitate (IP) ribosomes and their associated RNAs from the selected cell type.

In addition to the initial publication that developed the technique, several other laboratories have utilized the RiboTag model. Diverse tissues such as mouse Sertoli and Leydig cells<sup>15</sup>, microglia<sup>16</sup>, neurons<sup>17,18</sup>, oocytes<sup>19</sup>, and cultured cells<sup>20</sup> have been profiled and studied. Though this protocol is clearly able to successfully isolate ribosomes and the associated RNAs across a diverse tissue types there are still areas needing improvement, especially when applied to mutant systems. In particular, common reliance on fresh tissue results in increased technical variation which can greatly reduce the power of the analysis. Secondly, confident identification of differentially translated targets is made more challenging when high immunoprecipitation background occurs from non-*Cre* recombined cell types as previously reported<sup>13</sup>. While Sanz et al. engineered the basic premise of the technique, in this manuscript the Snyder laboratory presents optimization of the protocol to reduce these concerns, rendering the method more practical and efficient.

The intent of this article is to explain the steps for breeding mice expressing cell-specific HA-tagged ribosomes, immunoprecipitating these ribosomes from flash-frozen samples, and purifying their associated RNAs for further downstream analyses. As the mammalian male germ cell and the infertility mutation studied provide unique challenges, efforts have been made to illuminate ways this technique can be adapted to other cell systems.

## Protocol

All animal use and handling practices have been approved by Rutgers University's Internal Animal Care and Use Committee (IACUC).

### 1. Mouse breeding

- Breed female mice homozygous for an RNA binding protein mutation that leads to male infertility (manuscript in preparation, referred to herein as *the gene of interest*) in trio matings to males hemizygous for the *Stra8-iCre* allele (B6.FVB-Tg(*Stra8-iCre*)1Reb/LguJ) (*Cre*+), as pairing two females to every male increases breeding efficiency.  
NOTE: The mutant gene of interest (M) was passed maternally, as females homozygous for M have normal fertility. This has the added benefit of allowing paternal transmission of the male germ cell *Cre* (hemizygous), as recommended<sup>21</sup> and optimizing the percent of offspring with the desired allelic combination. Because homozygous *Cre*s exhibit germ cell toxicity<sup>22</sup>, it is recommended the allele be maintained and passed in a heterozygous or hemizygous state. Importantly, *Cre* expression must not co-occur with the *Rpl22-HA* allele until the experimental population. Failure to isolate the *Rpl22-HA* allele from *Cre* in breeding animals will result in offspring that *globally* express *Rpl22-HA* due to germ cell *Cre* activity. This issue is specific to germ cell. Additionally, the *Stra8-iCre* is specific to the authors' cell population of interest<sup>22</sup>, targeting cells transitioning into and very early in meiosis, including preleptotenes and leptotenes. A different *Cre* driver specific to another cell type of interest can be used instead. Common practice dictates male germ cell expressed *Cre*s be transmitted on the paternal side. However, it is possible maternal transmission of the *Stra8-iCre* will result in similar transgene expression in male offspring. Regardless of breeding scheme selected, in order to generate offspring with equivalent *Cre* expression, all experimental samples should be generated via *Cre* transmission from the same parental side (either always maternal or always paternal).
- Genotype resulting male pups as described in section 2.4. Select those carrying the *M* allele and positive for *Cre* (+/*M*:*Cre*+) for downstream breeding.
- Breed female mice homozygous for the *M* allele in trio matings to males homozygous for *Rpl22-HA* (B6J.129(Cg)-*Rpl22*<sup>tm1.1P<sup>sam</sup></sup>/SjJ).  
NOTE: The *Rpl22-HA* background is highly mixed, so care should be exercised when assessing strain-specific phenotypes.
- Genotype resulting female pups to identify those carrying the *M* allele and positive for *Rpl22-HA* (+/*M*:*Rpl22-HA*+) (see section 2.3). Select these females for downstream breeding.
- Cross +/*M*:*Cre*+ males with +/*M*:*Rpl22*+ females in trio matings. Genotype the resulting pups (see sections 2.3 and 2.4) to identify males that are both *Cre*+ and *Rpl22*+ and either wildtype or *M*/*M*.  
NOTE: As this work focuses on a mutation resulting in complete male infertility, special considerations have been taken in the breeding scheme to most efficiently obtain desired experimental genotypes. Such considerations may be unnecessary in other experimental models. See Figure 2 for a full breeding schematic and accompanying legend for additional discussion of breeding considerations.

### 2. Sample collection

- Collect testes from male mice at 21 days post-partum (dpp).
  - Sacrifice mice by CO<sub>2</sub> inhalation followed by cervical dislocation. Make a ventral incision (3 cm) on each animal flanked by two shorter (2 cm each), connected lateral incisions. Pull the skin and peritoneum back to reveal the testes.
  - Using forceps, pull the epididymal fat pad from one side of the body cavity to reveal the epididymis and testis. With tenotomy scissors, excise the testis, taking care to trim away epididymis, surrounding fat, and any external vasculature. Place intact testes in a clean 1.7 mL tube.

3. Repeat with other side, adding the second testes to the first tube. Cap this tube and immediately submerge it in liquid nitrogen to flash-freeze.  
NOTE: Samples can be preserved at -80 °C until use.
2. Collect additional tail tip samples for each animal (2 mm) for genotyping confirmation.
  1. To extract DNA, add 100 µL of 50 mM NaOH to a 2 mm tail tip in a 1.7 mL tube and boil at 95 °C for 30 min. Add 100 µL of 50 mM HCl and 20 µL of 1 M Tris-HCl pH 8.0 and centrifuge samples for 3 min at 10,000 x g. Retain supernatant (containing genomic DNA) and store extracted DNA at 4 °C until use as template for the following genotyping reactions.
3. Perform *Rpl22-HA* genotyping following a method adapted from Sanz et al.<sup>13</sup> using the following primers: forward: 5' GGGAGGCTTGCTGGATATG 3'; reverse: 5' TTTCCAGACACAGGCTAAGTACAC 3'.
  1. Prepare a reaction mixture consisting of 2 µL of DNA as extracted in step 2.2.1, 0.08 µL of 25 mM dNTPs, 0.1 µL of 10 mM forward primer, 0.1 µL of 10 mM reverse primer, 2 µL of a polymerase chain reaction (PCR) buffer (650 mM Tris pH = 8.8, 165 mM (NH<sub>4</sub>)<sub>2</sub>SO<sub>4</sub>, 30 mM MgCl<sub>2</sub>, and 0.1% Tween), 0.2 µL of *Taq* polymerase, and nuclease-free H<sub>2</sub>O to a total volume of 20 µL.
  2. Use the following thermocycler conditions: a 30 s primer melting step at 95 °C, 30 s anneal at 64 °C and a 30 s elongation at 72 °C, repeated 37 times with a final 5 min elongation at 72 °C.  
NOTE: This yielded a product size of 260 bp for wildtype samples and 292 bp for samples that were *Rpl22-HA*+
4. Perform *Cre* genotyping using the following primers: forward: 5' GTGCCAGCTGAACAACAGGA 3'; reverse: 5' AGGGACACAGCATTGGAGTC 3'. Prepare the PCR reaction as described in step 2.3.2 utilizing the *Cre* primers instead. Use the following thermocycler conditions: a 30 s primer melting step at 95 °C, 30 s anneal at 60 °C and a 15 s elongation at 72 °C, repeated 35 times with a final 5 min elongation at 72 °C.
5. Carry out gene of interest genotyping as is standard for the gene in question.  
NOTE: The author's genotyping protocol utilizes a concentrated custom *Taq*, and as such, other users may have to modify the conditions to suit their enzymatic requirements. In order to better understand the impact of this gene of interest's loss on translation, males that were either wildtype or homozygous for the mutant allele of interest and that were also *Cre*<sup>+</sup> and *Rpl22*<sup>+</sup> were selected to be the experimental samples. Genotype selection is further discussed above in section 1.

### 3. Preparation of solutions

NOTE: Preparation of solutions and all subsequent steps must be done under stringently conditions.

1. To prepare homogenization buffer (HB), add 2.5 mL of 1 M Tris pH 7.4, 5 mL of 1 M KCl, 600 µL of 1 M MgCl<sub>2</sub>, and 500 µL of NP-40 to a 50 mL tube. Bring to volume (50 mL) in diethyl pyrocarbonate (DEPC) H<sub>2</sub>O and mix until all components are incorporated.  
NOTE: The final concentrations will be as follows: 50 mM Tris pH 7.4, 100 mM KCl, 12 mM MgCl<sub>2</sub>, and 1% NP-40.
2. To prepare high salt wash buffer (HSWB), add 2.5 mL of 1 M Tris pH 7.4, 15 mL of 1 M KCl, 600 µL of 1 M MgCl<sub>2</sub>, and 500 µL of NP-40 to a 50 mL tube. Bring to volume (50 mL) in DEPC H<sub>2</sub>O and mix until all components are incorporated.  
NOTE: The final concentrations will be as follows: 50 mM Tris pH 7.4, 300 mM KCl, 12 mM MgCl<sub>2</sub>, and 1% NP-40. The protocol can be paused here, and solutions can be stored at room temperature until use.

### 4. Preparation of tissue

1. Preweigh all sample tubes, recording weight, and precool in liquid nitrogen.
2. Precool sterile mortar, pestle, and weighing spatula on dry ice.
3. Grind flash-frozen tissue samples to a fine powder using a precooled, sterile mortar and pestle on dry ice.
  1. Place flash frozen tissue into precooled mortar on dry ice. Gently break tissue into large pieces using pestle and grind slowly until tissue is a fine powder.  
NOTE: Although fresh tissue can also be used, as per the original protocol<sup>13</sup>, no significant difference in outcome is observed with the use of flash-frozen tissues. See Representative Results and Discussion for details.
  2. Carefully transfer ground sample to precooled collection tube by scraping powder from mortar using precooled spatula. Ensure only tissue is collected and not any moisture deposited onto the cold mortar.
  3. Weigh the tube with tissue, taking care to keep on dry ice whenever possible. Calculate the mass of tissue by subtracting initial weight of the tube from the weight of the tube with the sample in it. Record this value for later calculation of lysis buffer volumes.  
NOTE: The protocol can be paused here, and samples can be stored at -80 °C until use.

### 5. Homogenization of sample

1. Prepare lysis buffer (10 mL HB + supplements) by adding 10 µL of 1 M dithiothreitol (DTT), 1 protease inhibitor tablet, 50 µL of RNase inhibitor (40,000 units/mL), 200 µL of 5 mg/mL cycloheximide, and 100 µL of 100 mg/mL heparin to 10 mL of HB. Mix until all components are incorporated and keep on ice until use.  
NOTE: The final concentrations of the supplements in 10 mL HB will be as follows: 1 mM DTT, 200 U/mL RNase inhibitor, 100 µg/mL cycloheximide, and 1 mg/mL heparin. This solution must be used within 24 h of the addition of the supplements and can be kept at 4 °C or on ice until use.
2. For every 100 mg of sample, add 1 mL of lysis buffer. With the same pipette used to add the lysis buffer, carefully pipette the resulting lysate up and down to fragment cells and mix. Continue pipetting until the sample is no longer viscous, generally 25–30 strokes.  
NOTE: Because the solution is very viscous at first, a large diameter pipette should be used to mix the solution. A standard 1000 µL is normally sufficient for 100 mg of tissue.

3. Set samples on ice for 10 min to lyse. Then, spin samples in a precooled centrifuge (4 °C) for 10 min at 10,000 x g. A large, loose, cloudy pellet should form in the bottom of the tube.
4. Being careful not to disturb the pellet, collect the lysate into a new tube and record volume for each sample. To prevent sample degradation, ensure that samples remain cool throughout the remaining protocol, storing on ice or at 4 °C whenever possible.

## 6. Equilibration of beads

1. Using the volume of lysate from step 5.2, calculate the required volume of magnetic beads coupled to the appropriate antibody binding protein (in this case, protein G). For 1 mL of lysate, use 375 µL of protein G beads (30 mg/mL).  
NOTE: Choice of conjugated beads will vary with anti-HA antibody used; for example, if a rabbit-generated anti-HA antibody is selected, protein A beads will be preferable.
2. Using a magnetic tube rack, remove bead solvent and add an equal volume of fresh lysis buffer to the beads. Rotate 5 min at 4 °C to wash. Perform all rotation steps using a benchtop tube rotator set to 20 rpm.
3. Place the tube on the magnetic tube rack and remove the wash buffer.
4. Repeat steps 6.1–6.3 two more times.
5. Add lysis buffer at the original volume to equilibrated beads. Store at 4 °C or on ice until use.

## 7. Preclearing sample

1. Add 50 µL of equilibrated beads for every 1 mL of lysate to supernatant of lysed sample (lysate) and rotate at 4 °C for 1 h.
2. Place the tube on the magnet rack and collect lysate into a fresh tube. Discard used beads.
3. To the lysate add 25 µL of equilibrated beads for every 1 mL and rotate at 4 °C for 1 h. Store remaining equilibrated protein G beads at 4 °C overnight.
4. Place tube on the magnet rack and collect lysate into a fresh tube. Discard used beads. From the cleared lysate, retain 50 µL to act as sample input control. Store at -80 °C.  
NOTE: The input sample acts as a control representing the total RNA population of the sample, including RNAs associated with other cell types in the tissue, to be used during downstream analyses to correct for gene expression changes as a function of mutation.

## 8. Incubation of antibody

1. For every 1 mL of cleared lysate, add 5 µg of anti-HA antibody. To prevent sample loss, seal the tube cap with laboratory film. Rotate samples 16–18 h at 4 °C.  
NOTE: The antibody incubation time and concentration has not been optimized. The authors found an overnight incubation with 5 µg to be sufficient; however, it is possible that a shorter incubation or less antibody will be adequate, or that a longer incubation or more antibody will improve binding.

## 9. Incubation of beads

1. For every 1 mL of cleared lysate, add 300 µL of protein G beads. Reseal the tube cap with laboratory film and rotate for 2 h at 4 °C.

## 10. Washing of beads

1. Place the sample tube on the magnet rack to allow beads to separate from IPed lysate. Pipette off flow-through lysate and discard, retaining the beads.
2. Apply 800 µL of HSWB to beads and allow to rotate for 10 min at 4 °C. Place the sample tube on the magnet rack and allow beads to separate from wash. Remove and discard wash.
3. Apply another 800 µL of HSWB to beads. Close sample and allow to rotate for 5 min at 4 °C. Place the sample tube on the magnet rack and allow beads to separate from wash. Remove and discard wash.
4. Repeat step 10.3 once more.

## 11. RNA extraction

1. Place the sample tube on the magnet rack and allow beads to separate from wash. Pipette off and discard wash, retaining beads for RNA extraction. Add 3.5 µL of 14.2 M beta-mercaptoethanol (bME) to beads and mix by vortexing for 15 s.
2. Extract RNA using a commercial RNA purification kit, as per manufacturer's instructions. Elute sample in 30 µL of RNase free H<sub>2</sub>O.  
NOTE: Though the 10 µL/sample DNase treatment is optional for most kits, it is strongly encouraged. This optional cleanup step significantly reduces background, allowing for a more accurate final concentration. It is strongly recommended to use a kit that contains beta-mercaptoethanol (bME) in the lysis buffer. bME acts as an additional RNase inhibitor to prevent sample degradation during RNA isolation.
3. Store sample at -80 °C or analyze immediately.

## 12. Quantification and sample analysis

1. Using a UV-Vis spectrophotometer, quantify RNA concentration and preliminary quality.
2. Analyze quality of RNA extracted from samples via a bioanalyzer.

NOTE: The resulting RNA can then be used for RNA-sequencing or other downstream analyses such as northern blotting or quantitative reverse transcription PCR (qRT-PCR).

## Representative Results

Previous reports have suggested non-specific immunoprecipitation from cells lacking *Cre*<sup>14</sup>. In order to determine if this was the case in our modified protocol, IP efficiency was determined in samples derived from animals carrying both *Cre* and *Rpl22-HA* and animals carrying only one but not the other with the expectation that without both a *Cre*-driver and *Rpl22-HA*, immunoprecipitated RNA should be minimal. As shown in **Figure 3**, very little RNA is isolated from samples lacking either *Cre* or *Rpl22-HA* demonstrating the effectiveness of this protocol to reduce IP background and isolate genuine HA-tagged ribosome RNAs. Further, both *Cre*-only and *Rpl22-HA*-only samples represent suitable negative controls.

Given the potential for reagent source to significantly impact the efficiency of IP, a series of antibodies and RNA isolation protocols were tested (**Figure 4**) in *Cre* and *Rpl22-HA* positive samples. These results demonstrate reagent selection can have a significant impact on IP efficiency thus any changes to reagent selection should be done so with care.

In order to test this protocol in the context of an RNA binding protein mutant, wildtype-*Cre*+*Rpl22-HA*+ (wildtype) and *gene of interest*<sup>-/-</sup>-*Cre*+*Rpl22-HA*+ (*Gene of interest*<sup>-/-</sup>) testis were examined for the effectiveness of the RiboTag system to isolate ribosome associated RNA (**Figure 5**). When RNA concentration of wildtype input and IP was compared to *Gene of interest*<sup>-/-</sup> input and IP, no significant difference was seen between genotypes. For both genotypes, however, the input concentration was significantly higher than the IP concentration, indicating that there was more RNA in the input sample (**Figure 5B**). This result is expected, as not all the mRNAs present in the cell are associated with the ribosome at any given time, especially in the case of germ cells where RNAs may be transcribed long before they are translated.

In order to confirm the quality of the RNA samples sent for sequencing, samples were run on a bioanalyzer. RNA integrity numbers (RINs), normally calculated as the ratio of 28S and 18S rRNA peaks, were compared across samples. In total RNA pools, RIN values are expected to be near 10 with a higher RIN correlated to higher inferred sample integrity and quality. While the IP samples had lower RIN than the inputs, the RINs were still within an acceptable range and were not dependent on sample genotype (**Figure 5C**). The reduced RIN values for IPed samples are likely a result of RNA degradation though very minor given the relatively small decrease in average nucleotide length of analyzed RNAs. Given the length of the protocol and temperatures required for the immunoprecipitation some degradation is expected. It is also possible the reduced RIN and RNA length is a function of enrichment for non-rRNA species, such as mRNAs.

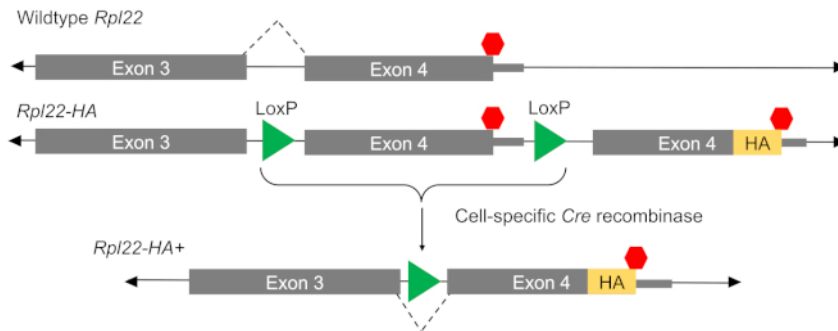


**Figure 1: The RiboTag method.** The premise of the method is biologically simple. A new Exon 4 is inserted into the sequence for the *Rpl22* locus downstream of the original Exon 4. In the presence of a *Cre* driver, loxP sites on either side of the original Exon 4 are cut, excising the floxed exon. The HA-tagged Exon 4 is now incorporated into *Rpl22* mRNA, generating an HA tagged RPL22 in cells expressing CRE. [Please click here to view a larger version of this figure.](#)

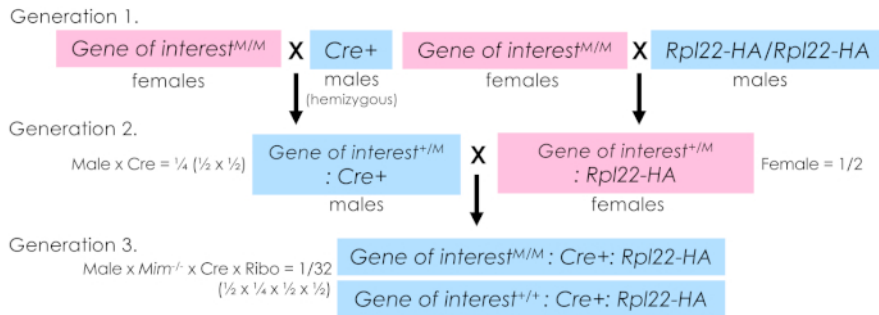


**Figure 2: Sample breeding scheme for RiboTag mice.** The breeding scheme used to generate experimental animals is shown. A two-pronged scheme was utilized. In generation 1, two parallel sets of breeder trios were established. One side combined the allele of interest (carried maternally as this specific mutation results in male infertility) with the hemizygous *Cre* and on the other combining the allele of interest, again carried maternally, with *Rpl22-HA*. Then, in generation 2, males from the first pairing that carry the allele of interest and the *Cre* are crossed to female offspring of the second pairing that carry the allele of interest and *Rpl22-HA*. The genotypes of the resulting offspring are determined, and experimentally relevant animals selected (in this case either wildtype or homozygous mutant carrying both the *Cre* and *Rpl22-HA* alleles). It is important to note for germ cell expressing *Cre*-drivers, the *Cre* and *Rpl22-HA* alleles should not be bred together until the experimental generation. Exposure of the *Rpl22-HA* allele to germ cell-expressed *Cre* in breeding generations will drive germ-cell *Rpl22-HA* excision. Any resulting offspring will globally express *Rpl22-HA* thus preventing cell-specific ribosome isolation. In the system described herein, an n = 4 per genotype provided sufficient statistical power for downstream analyses. Biological replicate number should be determined for each experimental system. [Please click here to view a larger version of this figure.](#)

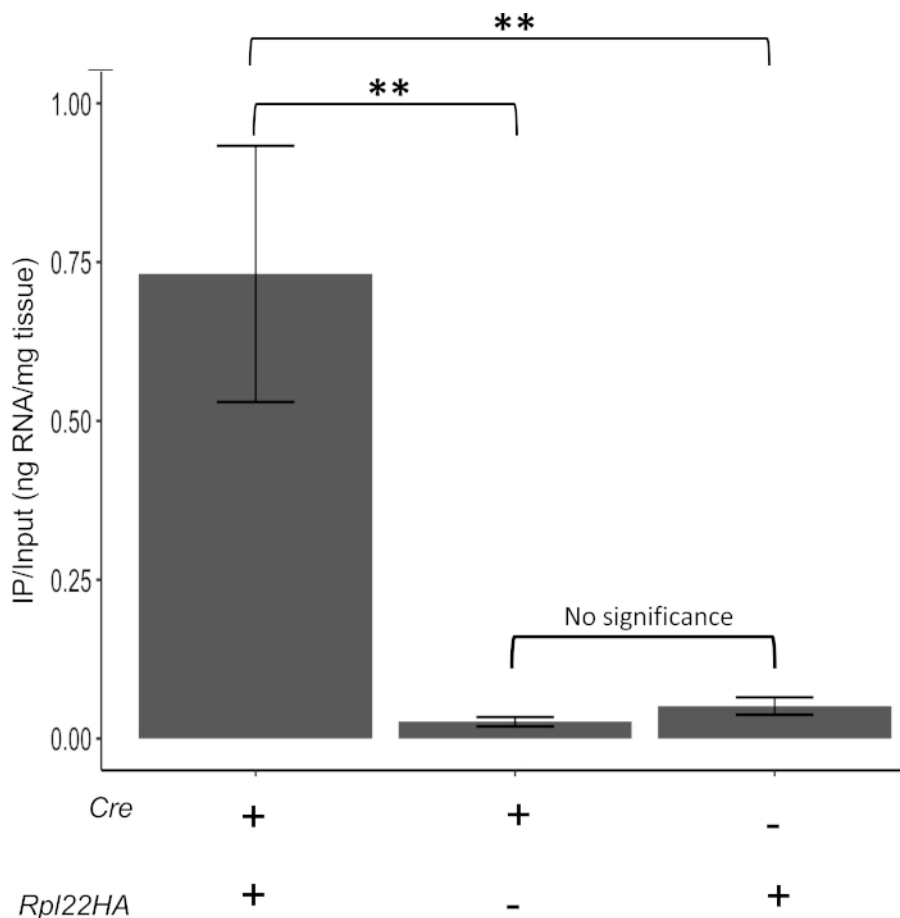


**Figure 3: Confirmation of negative controls.** Samples that are *Cre*<sup>+</sup> and *Rpl22-HA*<sup>+</sup> show higher RNA pulldown than samples that are *Cre*<sup>+</sup> or *Rpl22-HA*<sup>+</sup> alone. There is no significant difference between *Cre*<sup>+</sup> and *Rpl22-HA*<sup>+</sup> sample RNA pulldown efficacy, indicating that samples lacking either the *Cre* or the *Rpl22-HA* are suitable negative controls. A "+" indicates that the corresponding allele or transgene was present in these samples and a "-" denotes its absence. IP/input represents the ratio of RNA immunoprecipitated (IP) over total (input) RNA. Value calculated from concentration in nanograms. \*\* indicates p < 0.025. [Please click here to view a larger version of this figure.](#)

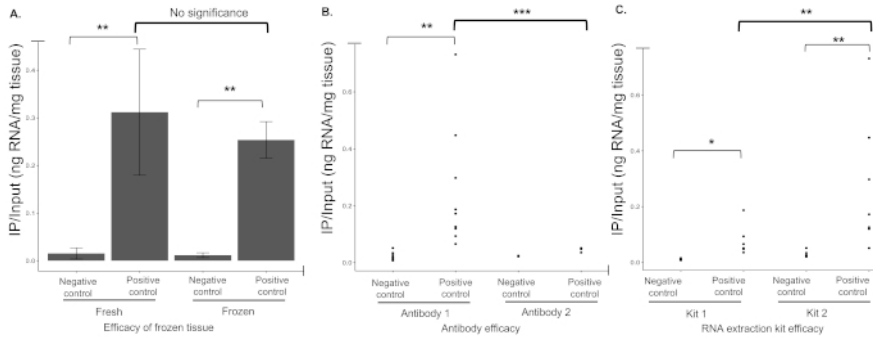


**Figure 4: Reagents impact protocol success.** (A) Flash frozen tissue results in immunoprecipitation efficiency similar to that of fresh tissue. (B) IP efficiency for two commercial antibodies were determined, designated as Antibody 1 and Antibody 2 (**Table of Materials**). When tested, Antibody 1 was more efficient at pulling down RNA than Antibody 2 which appeared to be unable to differentiate between negative (not expressing either *Cre* or *Rpl22-HA+*) and positive controls (expressing both *Cre* and *Rpl22-HA+*). Dots indicative of the ratio of IPed versus input RNA for individual biological replicates. (C) When RNA extraction kits (**Table of Materials**) were compared, Kit 2 significantly outperformed Kit 1. Though both kits IPed a similar amount of RNA from negative controls, Kit 2 resulted in a significantly higher RNA yield from positive samples. \* indicates  $p < 0.05$ , \*\*  $p < 0.025$ , \*\*\*  $p < 0.01$ . [Please click here to view a larger version of this figure.](#)

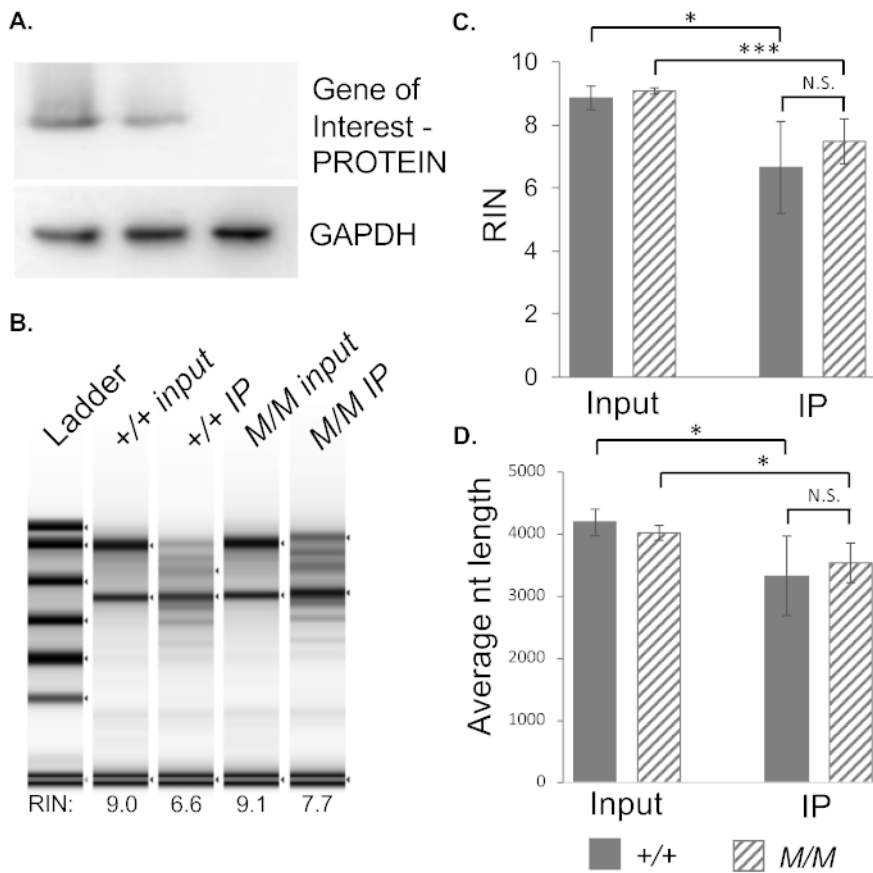


**Figure 5: Application of the method to a mutant model.** (A) Sample *Gene of interest* genotype confirmation via Western blotting using a custom in-house antibody against the *gene of interest* protein demonstrates *Gene of interest*<sup>-/-</sup> (*M/M*) males fail to produce the associated protein. GAPDH shown as a loading control. (B) Graphical bioanalyzer output from paired input and IPed samples for wildtype and mutant samples. (C) Comparison RNA integrity numbers (RIN) by sample type and genotype. (D) Average nucleotide length of RNA species analyzed by bioanalyzer by sample type and genotype. \* indicates  $p < 0.05$ , \*\*  $p < 0.025$ , \*\*\*  $p < 0.01$ , N.S. not significant. N = 4 per genotype. [Please click here to view a larger version of this figure.](#)

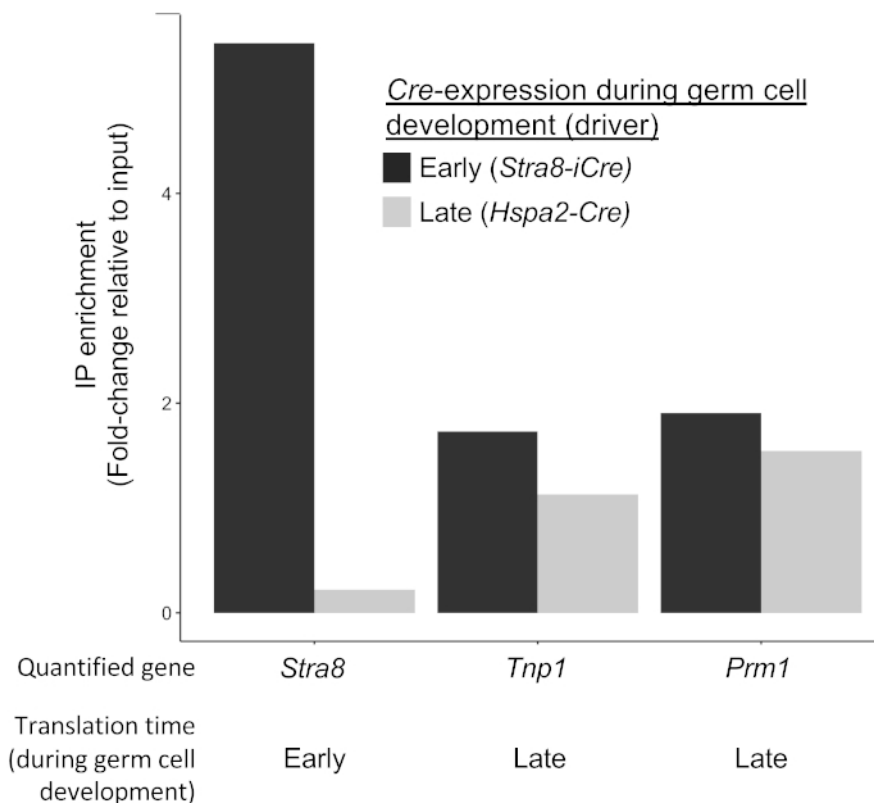


**Figure 6: Example of Cre driver confirmation.** Quantification of a gene translated early in germ cell development (*Stra8*) and two genes translated late in germ cell development (*Tnp1* and *Prm1*) analyzed by qRT-PCR of RNA immunoprecipitated from RPL22-HA driven by two different germ cell *Cres*, *Stra8-iCre* (expressed early in germ cell development) and *Hspa2-Cre* (expressed later in germ cell development, specifically after *Stra8* translation). Here, HA-IP of *Stra8* is achieved with the early germ cell *Cre* driver but not with the later germ cell *Cre* driver demonstrating cell-specificity of the immunoprecipitation. In contrast, HA-IP of transcripts translated in late germ cells is achieved by both *Stra8-iCre* and *Hspa2-Cre*. This is expected as cells that express *Stra8-iCre* will generate HA-tagged RPL22 throughout the entirety of their development while those expressing *Hspa2-Cre* will only do so during the later portions of their development. [Please click here to view a larger version of this figure.](#)

## Discussion

Understanding the translome of a particular cell type is invaluable for more accurately understanding a cell's physiology in the normal or mutant state. Special benefit is seen in systems wherein translation is uncoupled from transcription, such as in neural tissue where translation occurs very far from transcription, or in germ cells where transcription occurs long before translation. Relative to other methods of translome analysis, the RiboTag system's biggest advantage comes from the use of the *Cre* recombinase system. This allows the freedom to target any cell population that has a relevant *Cre* driver. Secondly, the RiboTag IP as described herein is effective and much less technically challenging and time-consuming than either polysome or ribosome profiling. Lastly, RiboTag IP can be easily performed at the benchtop.

There are a number of critical steps in this protocol. Chief among them is the establishment of the RiboTag mouse line and generation of experimental animals for study. As for all genetic models, careful tracking of individuals within the mouse colony as well as careful genotyping protocols should be applied. PCR genotyping as per Sanz et al. should include primers targeting the loxP site 5' of the wildtype exon 4 to distinguish between wildtype alleles (260 bp) and mutant (290 bp)<sup>13</sup>. For the case of RiboTag analysis in germ cell models, very specific breeding requirements should be adhered to. First, in the case of mutants that result in infertility, thoughtful breeding strategies should include methods to optimize the number of offspring with the desired genotype in intermediate and experimental generations. Second, in the case of germ cell specific *Cres*, care should be taken regarding *Cre*-zygosity given the sensitivity of germ cells to *Cre* toxicity. In the germ cell, high levels of *Cre* protein can have deleterious effects<sup>22</sup>, prohibiting the use of *Cre/Cre* animals in the breeding scheme. Lastly, when using germ cell *Cres*, it is important to isolate the RiboTag allele from the *Cre* until the final generation as *Cre* expression in the germ cell of an intermediate generation will result in offspring expressing *Rpl22-HA* globally.

Regardless of cell system, a number of recommended controls are possible to verify robustness of both *Cre* expression and specificity. Proper expression of your *Cre* and expected excision of *Rpl22-HA* can be determined using multiple methods. In the first, tissue isolated from experimental animals can be stained for HA using either immunohistochemistry or immunofluorescence<sup>15</sup>. This method is optimal in that it requires no *a priori* knowledge of translated mRNAs in the target cell types. The second method, an example of which is demonstrated in **Figure 6**, requires some knowledge of translationally regulated messages in the target cell types. In this method, enrichment for a known translationally regulated mRNA can be confirmed from the selected *Cre*-driver using quantitative PCR of IPed versus input RNA. Likewise, robust *Rpl22-HA* expression can be confirmed by comparison of *Cre+/Rpl22+* samples (positive controls) with either *Cre-/Rpl22+* or *Cre+/Rpl22-* samples

which act as effective negative controls (see **Figure 3**). These comparisons can either be done on total IPed RNA or enrichment for a known translationally regulated mRNA assessed by qRT-PCR or some other quantitative method.

Common problems in the execution of the protocol tend to only become apparent when RNA yield is unexpectedly low or high. The most common cause for these failures arise from incorrect genotyping of individuals. We recommend retaining additional tissue from collected sample to confirm genotypes of all samples in the case of unexpected RNA yields. Once confirmed, other possibilities should be considered including the possibility of RNase contamination or sample degradation. Careful sample storage and handling and maintenance of RNase free zones within the laboratory can greatly reduce or eliminate these issues. Although RNA isolation issues are another potential problem in this protocol, the use of commercial kits greatly reduces this issue though care should be taken to ensure they are maintained as RNase free and contain no expired solutions. Lastly, as with all antibody-based procedures, variations in lot, storage conditions, concentration, or even shipping have the potential to negatively impact the quality of the antibody and the subsequent success of the pulldown. As a result, following careful and repeated testing, we chose the most consistent and efficient antibody available.

This protocol contains two major modifications relative to other published RiboTag protocols that significantly enhance the likelihood of success. One is the ability to use flash frozen tissue, thereby mitigating any issues involving lot, technician, or technical run variations. Samples can be collected and stored allowing isolation of HA-ribosomes from all samples at once, lowering what may be major sources of variation. Second, the addition of the preclear step substantially reduces the sort of background reported by other users of the RiboTag system. Recently, a protocol report by Sanz et al. indicates the presence of high background due to abundance of ribosome-associated transcripts from non-*Cre*-driven cells<sup>14</sup>. Our protocol remedies this issue by including a preclearing step, effectively eliminating the presence of RNA in *Cre* negative IP samples.

Like all systems, the inherent limitations of the RiboTag system should be kept in mind. When using uncharacterized *Cre* drivers, analysis of expression should be performed prior to experimental sample production. From the perspective of translation, several nuances of this method should be noted. First, RiboTag does not allow differentiation between mRNAs poised to translate and those actively translating. As such, current RiboTag-based methods do not allow the quantification of translation efficiency as a function of individual mRNAs. If translation efficiency is of interest, it may be measured on a cell-specific basis if the RiboTag method is combined with other translome analysis tools such as polysome profiling. Secondly, it is fundamental to take into account total RNA abundance changes stemming from individual or genotype dependent variance. It is for this reason that careful isolation of input RNA accompany immunoprecipitation and samples derived from each remain paired throughout any downstream analyses. Lastly, and in regards to RiboTag-based analysis, it should be remembered that association with a ribosome does not necessarily prove translation is occurring. Secondary methods of analysis should be performed to confirm translational regulation in targets of interest.

This protocol describes the isolation of ribosome-associated RNAs from the germ cells of male mice using the RiboTag model. Not accounting for mouse breeding and sample collection, the protocol takes two days, with three hours the first day, best done in the afternoon, an overnight incubation, followed by five hours of work the subsequent morning. It is strongly recommended that preparation of stock solutions (HB and HSWB) as well as tissue grinding be done in advance. The overall success of the protocol is reliant on correct genotyping and stringently RNase-free conditions. The ability to examine the translome of specific cell types will allow future studies to better understand the relationship between transcription, translation, and the proteome in myriad cell types and mutant backgrounds.

## Disclosures

The authors have nothing to disclose.

## Acknowledgments

This work was funded by NIH grant NICHD R00HD083521 to EMS and internal support from Rutgers University to EMS.

## References

1. Snyder, E. M. et al. Gene expression in the efferent ducts, epididymis, and vas deferens during embryonic development of the mouse. *Developmental Dynamics*. **239** (9), 2479-2491 (2010).
2. Snyder, E. M., Small, C. L., Li, Y., Griswold, M. D. Regulation of gene expression by estrogen and testosterone in the proximal mouse reproductive tract. *Biology of Reproduction*. **81** (4), 707-716 (2009).
3. Iguchi, N., Tobias, J. W., Hecht, N. B. Expression profiling reveals meiotic male germ cell mRNAs that are translationally up- and down-regulated. *Proceedings of the National Academy of Sciences of United States of America*. **103** (20), 7712-7717 (2006).
4. Busada, J. T. et al. Retinoic acid regulates Kit translation during spermatogonial differentiation in the mouse. *Developmental Biology*. **397** (1), 140-149 (2015).
5. Kleene, K. Patterns of translational regulation in the mammalian testis. *Molecular Reproduction and Development*. **43** (2), 268-281 (1996).
6. Mali, P. et al. Stage-specific expression of nucleoprotein mRNAs during rat and mouse spermiogenesis. *Reproduction Fertility and Development*. **1** (4), 369-382 (1989).
7. Steward, O., Schuman, E. M. Protein synthesis at synaptic sites on dendrites. *Annual Review of Neuroscience*. **24**, 299-325 (2001).
8. Michel, A. M., Baranov, P. V. Ribosome profiling: a Hi-Def monitor for protein synthesis at the genome-wide scale. *Wiley Interdisciplinary Reviews: RNA*. **4** (5), 473-490 (2013).
9. Snyder, E. et al. Compound Heterozygosity for Y Box Proteins Causes Sterility Due to Loss of Translational Repression. *PLoS Genetics*. **11** (12), e1005690 (2015).
10. Pringle, E. S., McCormick, C., Cheng, Z. Polysome Profiling Analysis of mRNA and Associated Proteins Engaged in Translation. *Current Protocols in Molecular Biology*. **125** (1), e79 (2019).
11. McGlincy, N. J., Ingolia, N. T. Transcriptome-wide measurement of translation by ribosome profiling. *Methods*. **126**, 112-129 (2017).

12. Aeschimann, F., Xiong, J., Arnold, A., Dieterich, C., Grosshans, H. Transcriptome-wide measurement of ribosomal occupancy by ribosome profiling. *Methods*. **85**, 75-89 (2015).
13. Sanz, E. et al. Cell-type-specific isolation of ribosome-associated mRNA from complex tissues. *Proceedings of the National Academy of Sciences of United States of America*. **106** (33), 13939-13944 (2009).
14. Sanz, E., Bean, J. C., Carey, D. P., Quintana, A., McKnight, G. S. RiboTag: Ribosomal Tagging Strategy to Analyze Cell-Type-Specific mRNA Expression In Vivo. *Current Protocols in Neuroscience*. **88** (1), e77 (2019).
15. Sanz, E. et al. RiboTag analysis of actively translated mRNAs in Sertoli and Leydig cells in vivo. *PLoS One*. **8** (6), e66179 (2013).
16. Haimon, Z. et al. Re-evaluating microglia expression profiles using RiboTag and cell isolation strategies. *Nature Immunology*. **19** (6), 636-644 (2018).
17. Ceolin, L. et al. Cell Type-Specific mRNA Dysregulation in Hippocampal CA1 Pyramidal Neurons of the Fragile X Syndrome Mouse Model. *Frontiers in Molecular Neuroscience*. **10**, 340 (2017).
18. Puighermanal, E. et al. drd2-cre:ribotag mouse line unravels the possible diversity of dopamine d2 receptor-expressing cells of the dorsal mouse hippocampus. *Hippocampus*. **25** (7), 858-875 (2015).
19. Chen, J. et al. Genome-wide analysis of translation reveals a critical role for deleted in azoospermia-like (Dazl) at the oocyte-to-zygote transition. *Genes and Development*. **25** (7), 755-766 (2011).
20. Lesiak, A. J., Brodsky, M., Neumaier, J. F. RiboTag is a flexible tool for measuring the translational state of targeted cells in heterogeneous cell cultures. *Biotechniques*. **58** (6), 308-317 (2015).
21. The Jackson Laboratory. *B6.FVB-Tg(Stra8-icre)1Reb/LguJ*. (2019).
22. Bao, J., Ma, H. Y., Schuster, A., Lin, Y. M., Yan, W. Incomplete cre-mediated excision leads to phenotypic differences between Stra8-iCre; Mov10l1(lox/lox) and Stra8-iCre; Mov10l1(lox/Delta) mice. *Genesis*. **51** (7), 481-490 (2013).